Hindawi
International Journal of Photoenergy
Volume 2022, Article ID 8790631, 17 pages
https://doi.org/10.1155/2022/8790631

Research Article

Modeling and Simulation of Solid Oxide Fuel Cell Integrated with Anaerobic Digester, Thermal Storage Unit and Solar Collector: A Net Zero Emission System

Muhammad Nihal Naseer,[1,2] **Khurram Kamal**,[1] **Muhammad Abid**,[3] **Asif Iqbal**,[3] **Hamdullah Khan**,[1] **Ch. Muhammad Zubair**,[1] **Sagar Kumar**,[1] **Tahir Abdul Hussain Ratlamwala**,[1] **and Malik Muhammad Nauman**[3]

[1]*National University of Sciences and Technology, Islamabad44000, Pakistan*
[2]*Faculty of Chemistry, Warsaw University of Technology, Noakowskiego 3, Warsaw 00-664, Poland*
[3]*Department of Energy Systems Engineering, Faculty of Integrated Technologies, University Brunei Darussalam, Bandar Seri Begawan, Brunei Darussalam*

Correspondence should be addressed to Muhammad Abid; mabid42@gmail.com

Received 3 February 2022; Revised 20 September 2022; Accepted 21 October 2022; Published 21 November 2022

Academic Editor: P. Davide Cozzoli

Energy production from clean and green sources is one of the eminent challenges to mankind. Overall, all industrial sectors contribute to CO_2 emission, but the energy production sector is a major contributor. In recent years, CO_2 emissions from the energy sector have increased by 1.7%. Therefore, the development of alternative energy production sources is a pivot for researchers. In this regard, the fuel cell has been a promising technology but still accompanied by the release of greenhouse gasses but relatively lower than that of fossil fuels. The integration of the fuel cell to the biogas has been a promising factor to reduce emissions. This study contributes to the same by producing a self-sustaining biogas-fuel cell multigeneration system for cold areas. Mathematical modeling of all complements of the system, i.e., anaerobic digester, solid oxide fuel cell, solar collector, and thermal storage system, is provided. MATLAB/Simulink environment is used for simulation of the system. The proposed system will use an anaerobic digester for methane production. Hence, produced methane will be used to power solid oxide fuel cell. The electricity of the fuel cell will power the residential place, and the thermal potential of the exhaust will be stored. In daylight, the solar thermal potential will be utilized for district heating. In the absence of solar light, stored thermal energy will be used for district heating and hot water supply. Additionally, the CO_2 emitted from the system will not be released into the environment but stored for industrial purposes. The best area of application of the proposed system is cold areas such as Switzerland.

1. Introduction

The ever-increasing population and industrial revolution have resulted in enormous waste production over the span of the last few years. On average, a person produces 2.22 kg of municipal waste every day. In 2016, only in South Asia, 334 million tons per year were generated, but this amount will hit the margin of 446 and 661 million tons per year in 2030 and 2050. Similarly, East Asia and the Pacific were on 468 million tons but are forecasted to increase to 602 and 714 million tons by 2030 and 2050. In nutshell, global waste production will increase by 26.72% by 2030 and 68.62% by 2050 [1]. Therefore, a sustainable destination to waste is an eminent issue. In this regard, various technologies are proposed such as waste to energy conversion, extraction of metals from waste, and many others [2–6]. Methane production from an anaerobic digester (AD) is also a promising technology that ensures a sustainable destination to waste

[7]. But this process is associated with CO_2 production. Therefore, such integrations are required that make this AD process an environment-friendly process [8, 9].

To sustain on this planet, a reduction in CO_2 emission is necessary as it is a major contributor to global warming [10]. There are other gasses present in the atmosphere, contributing to global warming, but CO_2 is a major contributor. It has the highest (RF) radioactive forcing factor among others. High RF depicts the high potential of gas to absorb solar radiation [11]. Despite the familiarization with the destructive nature of CO_2, it is still released into the environment in excessive amounts. The energy production system is a major contributor to this excessive release. The increasing energy demand made CO_2 emissions hit a margin of the historically high value of 33.1 Gt in 2018 [12]. Therefore, energy production from clean and green sources is important. In this regard, AD is integrated with SOFC to produce green energy and reduce emissions.

Various organic feeds can be used to produce methane, as depicted in Table 1 [13, 14]. Among various technologies, biofuel or methane production from AD process is preferred as evident from the literature [15]. Additionally, its implication for a broad waste type also increases its vitality for the research community.

The integration of different existing technologies has been of keen interest to the research community [16, 17]. Due to the intermittent nature of most renewable energy sources, integration has become a prime concern to ensure the seamless availability of green energy. For example, solar energy is only available during the daytime, so a system relying only on solar energy may not have an energy supply during night time. Therefore, another renewable energy source such as solar, biomass, or any other is integrated to ensure a smooth supply of energy. In a nut shell, the integration of green energy systems is compulsory for a smooth supply of energy [18].

The integration of fuel cell and biogas can provide the best solution for green energy production. The energy produced by the fuel cell is often accompanied by a release of CO_2 but relatively less than that of fuel cell. But this resealed amount of excess gasses can also be reduced by integrating fuel cell and biogas production [19]. Staniforth and Kendall [19] introduced a solid oxide fuel cell (SOFC) powered by biogas. This system [19] was operated and tested using different levels of carbon dioxide. It was observed that the high content of the CO_2 was beneficial for the integration of both as the internal reforming process was favored by the presence. On the other hand, a substantial issue was reported. The excess amount of carbon caused an issue by deposition. This deposition contaminates the electrode of fuel cell. Overall, it was observed that the performance of biogas integrated SOFC is comparable to that of hydrogen-integrated SOFC [19, 20]. But an issue of biogas production quality also causes an issue as using different types of biogas sources may alter the fuel cell life and overall efficiency [19].

As an alternative to distributed power generation, a novel approach was introduced by combining SOFC and gas turbine which is a cogeneration system further integrated with transcritical carbon dioxide cycle, and a mathematical model based on thermodynamics perspective (energy and exergy) is used to analyse it [21]. For optimizing the process, a multiobjective approach is adopted to determine optimized design parameters. The main optimization goals of this study were to increase energy efficiency, reduce cost, and optimize exergy efficiency. The performance of effects of SOFC at inlet temperature and current density was studied, and under the given conditions, the system achieved a 64.40% thermal efficiency, 62.13% exergy efficiency, and 446.28 kW power output. The conclusions that we obtained are with an increase in inlet temperature of SOFC thermal efficiency, and exergy efficiency can be increased. Additionally, an increment in current density results in a reduction in efficiencies. Using the NSGA-II algorithm shows that at maximum efficiency, there is minimum economic cost and vice versa. 63.08% was optimal thermal efficiency with a cost of 1.952 dollar/second and 61.1% optimal exergy efficiency with a cost of 1.920 dollar/second, and it has further room for improvement through optimization [21].

Two different cogeneration plants with different arrangements are compared; one is solid oxide fuel with internal reforming (IR-SOFC), and the other is a solid oxide fuel cell with external reforming (ER-SOFC) in power production and thermodynamic properties [22]. The design was optimized using an evolutionary algorithm (genetic algorithm) which is a multiobjective optimization method and parameters such as inlet SOFC temperature, current density fuel

Table 1: Different sources for biogas production adopted from the literature [13, 14].

Sources	Biogas production (m^3)
Cow manure	25
Pig manure	30
Whey	35
Potato slurry	39
Cow dung	45
Pig dung	60
Leaves of beets	70
Potato husk	74
Chicken dung	80
Sugar beet	90
Beer residue	120
Garden residue	175
Grass silage	185
Maize silage	190
Plant silage	195
Industrial fat	250
Food waste	265
Molasse	315
Old bread	500
Press cake residue	600
Bakery waste	714
Food fats	961

utilization factor, and steam-to-carbon ratio that were purposed as design parameters. There were two primary objectives for this study: first is to find maximum exergy efficiency, and the second is to minimize the CO_2 gas emission (EMI) vale simultaneously. Based on the results, the exergy value of IR-SOFC is about 9.6% higher than that of ER-SOFC. Also, the CO_2 gas emission (EMI) is also about 1.4% lower in IR-SOFC than that of ER-SOFC [22].

This gas-electricity cogeneration system is to produce clean and efficient electricity using the direct carbon solid oxide fuel cells which is a more promising material than solid carbon fuel [23]. A tubular 2-cell DC-SOFC is constructed by integrating symmetrical Ag-GDC electrodes. It has on par electrical output performance when hydrogen fuel is used in the same cell. It also produces electricity and CO when fueled with biochar. The electrical power output was observed under a constant current discharge of 0.25 A. The SOFC operating temperature is at maximum power density, open-circuit voltage, 800°C, 193 mW cm^{-2}, and 2.06 V, respectively. This system is relatively stable because of biochar [23].

Marechal et al. [24] introduced an integrated system of biogas and fuel cell. Biogas was produced from sewage sludge using an anaerobic digester and was fed to SOFC. This model was able to produce 100 kW of electricity. Trendewicz and Braun [25] attempted to provide technoeconomic analysis of such integrated systems. This study explored the systems in which biogas was recovered from waste. From the literature review, it was observed that usually, the amount of electricity produced from these systems was 300 kWe to 6 MWe.

As this study mainly focuses to ensure district heating and hot water for residential/industry, specifically for cold areas such as Switzerland where heating is needed all the year, some relevant studies are included. In the study [26], the amount of thermal energy consumed for process heating in Swiss industries was determined. The industries, in which process heat consumption was low and the requirement could be met by solar heating, were sorted out. For different regions of Switzerland, theoretical calculations of solar heating systems were done for promising industrial sectors and having a high potential for implementation. As per the conclusion, the main industries that have implementation potential are food, textile and clothing, chemistry and pharma, and paper. The data shows for the year 2016, these four industries consumed 33 PJ accounting 22% of Swiss industry energy consumption in that year. 12.1 PJ of that could be replaced by implementing solar heating systems, resulting in 8% Swiss industry energy consumption for 2016. It is pertinent to mention that the above process of heating calculations is done for processes occurring below 100°C, and other energy consumption where process heat is provided by electricity is neglected. However, solar heating can be used for the process occurring up to the temperature of 400°C, and if all those neglected areas are taken into consideration, solar heating can replace a huge portion of energy consumption.

In this study, the performance of a thermal system with dimensions 125*110 m^2, with a water flow length of 15.9 m, was investigated for flat plate collector solar heating. The study was done with two different flow rates, and results showed that heating at a lower flow rate, i.e., 5.3 L/min reached a temperature of 51.4°C as compared to heating at a flow rate of 6.51 L/min, reached a lower temperature of about 49°C. It was suggested that systems can be used for building or in-house purposes [27].

The aim of the study [28] was to examine the feasibility of tank thermal energy storage (TTES) for decarbonizing heating. Hourly heat flows with four different configurations were simulated in dwellings of 50 and 200 in Geneva in Switzerland. The four simulated configurations for heating were an oil boiler, a system with an air-water heat pump, a solar collector with TTES only, and solar collected with TTES and heat pump. The configurations were tested for performance based on parameters such as heat of cost, percentage of RES, decarbonization cost, and peak electricity load. Results show that although the air-water heat system has the benefits of low heating cost and a high percentage of RES, it does not eliminate CO_2 emission and has a high peak electricity load. However, a TTES is a better option if CO_2 emissions are of more concern, and it decarbonizes heating completely but at a higher cost. The peak electricity load is also low and has a good percentage of RES. These days, many researchers are working on optimizing TTES and conducting technoeconomic analyses to integrate it with renewable energy sources [29–31].

Further, there is a need to conduct modeling and simulation of energy systems using modern tools such as MATLAB. It allows users to conduct different analyses such as sensitivity analysis and perform optimization of the most impactful parameters.

This study proposes a novel multigeneration system by integrating an anaerobic digester with SOFC, CO_2 storage unit, thermal storage unit, and solar collector to ensure district heating and hot water supply all the year in an environmentally friendly manner. The proposed multigeneration system is simulated in MATLAB/Simulink platform which in itself is a novelty. Solar collector provides energy during the daytime, but during the night, thermally stored excess heat of SOFC does the trick. Electricity is also produced along with methane production for transport fuel applications. Moreover, the released CO_2 is not emitted into the atmosphere but stored for industrial purposes.

2. System Description

The proposed system integrates four technologies; anaerobic digestion (AD), solid oxide fuel cell (SOFC), thermal storage, and solar heating. The anaerobic digester works on provided manure and generates methane that is fed to SOFC. The electricity produced by SOFC is provided to the residential area, CO_2 is stored for selling to industry, and the excess heat is stored and released on a time of need. During the daytime, all the heat released from SOFC is stored, and solar heat is used for district heating or providing hot water. During the night, excess heat of SOFC is stored and simultaneously utilized for district heating. The proposed model

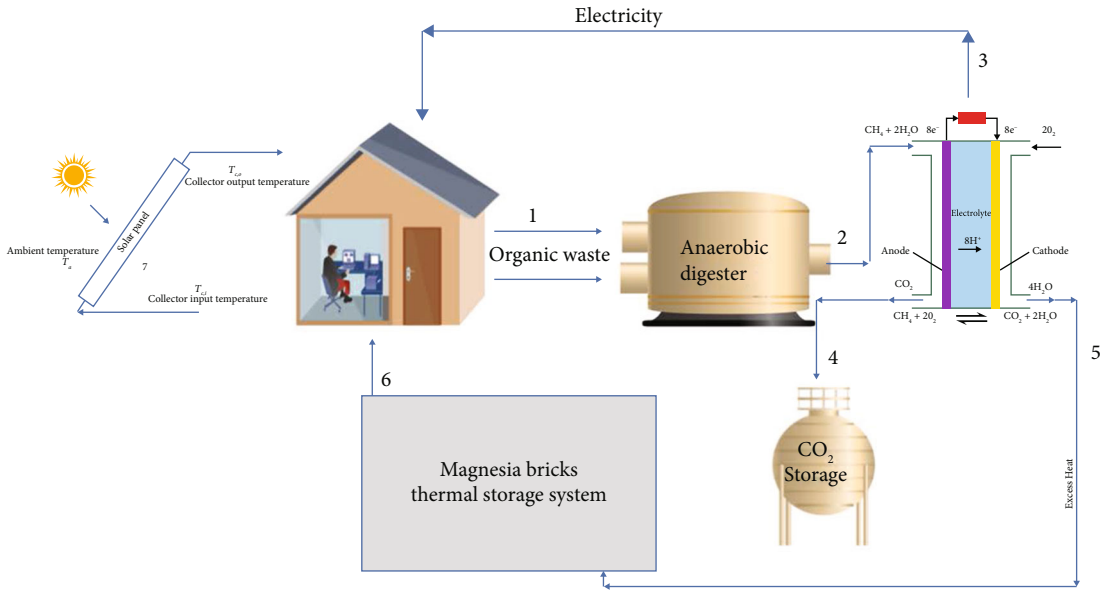

Figure 1: Proposed system: day cycle (1, 2, 3, 4, 5, and 7) and night cycle (1, 2, 3, 4, 5, and 6).

ultimately promises to provide electricity and heating to residential and CO_2 to industry, as depicted in Figure 1.

3. Mathematical Modeling

For ease of comprehension, the proposed model is divided into four parts: (i) AD, (ii), SOFC, (iii) solar heating, and (iv) thermal storage. The mathematical models used for simulation are described in the following subsections. The list of symbols used in modeling the system is provided in Table 2.

3.1. Anaerobic Digester. The process of generating methane from organic waste in the absence of oxygen by implication of microorganisms is referred to as anaerobic digestion. It is a renewable energy source that not only contributes to energy production but also provides a sustainable destination to waste [32]. The process of anaerobic digestion is mainly divided into four components: hydrolysis, acidogenesis, acetogenesis, and methanogenesis [32–34]. Various models are present in the literature for mathematical modeling of the AD process. Modified Hill's method (MHM) is adopted for this study [35–37].

3.1.1. Hydrolysis. The organic matter usually consists of large molecular chains, called polymeric chains. These chains are not directly accessible to microorganisms for exploiting their energy potential. Therefore, these high molecular weight chains are broken down to the lower molecular weight sugars [38]. The process of breaking large chain molecules is called hydrolysis. The MHM equation of the process is depicted in [35–37]

$$\frac{d(S_b)}{dt} = \left(S_{b_{\text{in}}} - S_b\right)\frac{F_{\text{feed}}}{V} - \frac{\mu_m K_1 X_{\text{acid}}}{K_s/S_b + 1}, \quad (1)$$

where μ_m is given as $\mu_m = 0.013T_{\text{reaction}} - 0.129$ and $20 \circ C \leq T_{\text{reaction}} \geq 60 \circ C$ [35-37].

3.1.2. Acidogenesis. This process converts monomers of organic waste into volatile fatty acids. The process of acidogenesis can be best understood by the method of souring milk [39]. The MHW equation of this process is as follows [35–37, 40].

$$\frac{d(S_v)}{dt} = \left(S_{v_{\text{in}}} - S_v\right)\frac{F_{\text{feed}}}{V} + \frac{\mu_m K_2 X_{\text{acid}}}{K_s/S_b + 1} - \frac{\mu_{mc} K_3 X_{\text{meth}}}{K_{sc}/S_v + 1}. \quad (2)$$

3.1.3. Acetogenesis. In this process, acetogenic bacteria converts previously generated volatile fatty acids to acetic acids. CO_2 and H_2 are the byproducts of this process [41]. The process adopted in this stage is hydrogenation. The HMW equation of this process is as follows [35–37].

$$\frac{d(X_{\text{acid}})}{dt} = \left[\frac{\mu_m}{K_s/S_b + 1} - K_d - \frac{F_{\text{feed}}}{bV}\right]X_{\text{acid}}. \quad (3)$$

3.1.4. Methanogenesis. This is the last step in the AD process in which methane is produced from acetic acids. The HMW equation of this process is as follows [35–37, 40].

$$\frac{d(X_{\text{methane}})}{dt} = \left[\frac{\mu_m}{K_{sc}/S_v + 1} - K_{dc} - \frac{F_{\text{feed}}}{bV}\right]X_{\text{methane}}. \quad (4)$$

3.1.5. Total Methane Produced. The total amount of methane produced in the process can be approximated by

$$F_{\text{meth}} = V\mu_c k_5 X_{\text{methane}}. \quad (5)$$

Table 2: List of symbols.

Symbol	Parameter	Unit
Anaerobic digester		
S_b	Concentration of organic matter	Kg m^{-3}
S_v	Concentration of volatile fatty acids	Kg m^{-3}
X_{meth}	Methanogen concentration	Kg m^{-3}
X_{acid}	Acidogen concentration	Kg m^{-3}
F_{feed}	Flow rate of feed	m^3 day^{-1}
V	Reactor volume	m^3
μ_m	Methanogen growth rate	Day^{-1}
μ_{mc}	Acidogen growth rate	Day^{-1}
K_1	Yield factor for hydrolysis	Constant
K_2	Yield factor for acidogenesis	Constant
K_3	Yield factor for methane gas production	Constant
K_s	Acidogenic Monod half velocity constant	Kg m^{-3}
K_{sc}	Methanogenic Monod half velocity constant	Kg m^{-3}
b	Retention time factor	Constant
Solid oxide fuel cell		
E	Open circuit voltage	V
N	Number of fuel cell	
E^o	Standard reversible voltage	V
R	Universal gas constant	J Mol^{-1} K
T	Operating temperature	K
F	Faraday constant	C Mol^{-1}
pH_2	Partial pressure of hydrogen	Pa
pO_2	Partial pressure of oxygen	Pa
pH_2O	Partial pressure of water	Pa
KH_2	Valve molar constant for hydrogen	Mol s^{-1} atm^{-1}
qH_2	Flow rate of hydrogen	m^3 s^{-1}
K_r	Constant	Mol s^{-1} A
I_f	Fuel cell current	A
U_{opt}	Optimum fuel utilization	Constant
r_{OH}	Ratio to H_2 to O_2	Constant
τ	Response time	S
Solar collector		
$T_{c,o}$	Collector outlet temperature	°C
T_a	Ambient temperature	°C
k_{aw}	Heat transfer coefficient absorber and atmosphere	W m^{-2} k^{-1}
k_{mw}	Heat transfer coefficient working fluid and atmosphere	W m^{-2} k^{-1}
A_{solar}	Area of solar panel	m^2
c	Specific heat of working fluid	J kg^{-1} K^{-1}
q	Mass flow rate of working fluid	Kg s^{-1}
I	Solar irradiance	W m^{-2}
η	Solar collector efficiency	
k	Heat transfer coefficient of solar collector	W m^{-2} k^{-1}
ρ	Density of working fluid	Kg m^{-3}
V_{wf}	Volume of working fluid	m^3
Thermal storage		
Q_{store}	Heat stored	J
T_f	Final temperature range of medium	K
T_i	Initial temperature range of medium	K
m	Mass of storage medium	Kg
c	Specific heat of storage medium	J kg^{-1} K^{-1}

3.2. Solid Oxide Fuel Cell. Different fuel cells are characterized by the type of material used in their electrode. As SOFC has ceramic or solid electrodes hence called SOFC. SOFC voltage is given by

$$V_{sofc} = N(E - V_{act} - V_{conc} - V_{ohm}). \quad (6)$$

3.2.1. Nernst Voltage. The reversible open circuit voltage of SOFC is given by the Equation (7). Equations (8)–(12) provide the necessary parameters to perform calculations of

$$E = \left\{ E^o - \frac{R.T}{2F} \ln\left(\frac{pH_2 \cdot \sqrt{pO_2}}{pH_2O}\right)\right\}, \quad (7)$$

where

$$pH_2 = \left(\frac{1/KH_2}{1 + \tau_{H_2} s}\right)\left(qH_2 - 2K_r I_f\right), \quad (8)$$

$$pO_2 = \left(\frac{1/KO_2}{1 + \tau_{O_2} s}\right)\left(qO_2 - K_r I_f\right), \quad (9)$$

$$pH_2O = \left(\frac{1/KH_2}{1 + \tau_{H_2O} s}\right)\left(2K_r I_f\right). \quad (10)$$

Moreover, qH_2 and qH_2O are given as following.

$$qH_2 = \frac{2K_r}{U_{opt}}\left(\frac{1}{1 + \tau_{H_2} s}\right), \quad (11)$$

$$qO_2 = \frac{qH_2}{r_{OH}}. \quad (12)$$

3.2.2. Activation Loss. The activation energy accompanies losses due to both chemical and electrical reactions [42]. The cathode has comparatively high activation polarization than

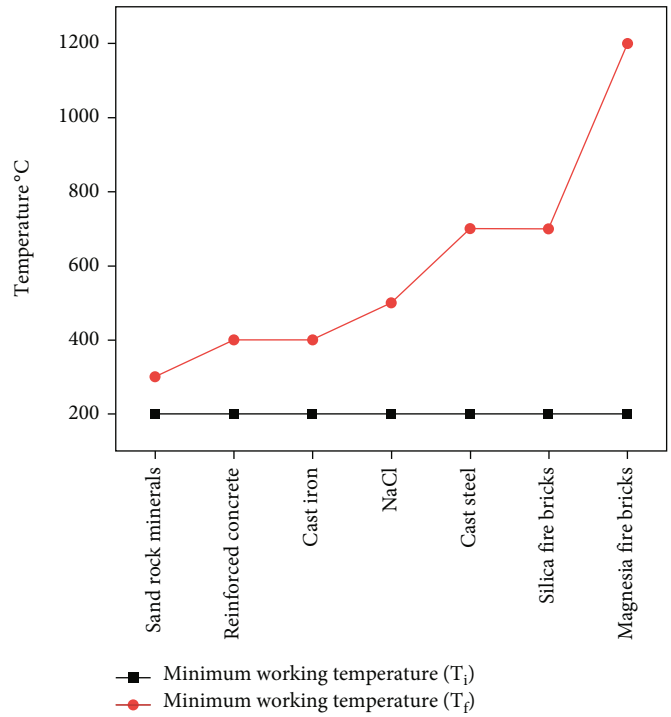

Figure 2: Temperature range of various thermal storage mediums [46, 50].

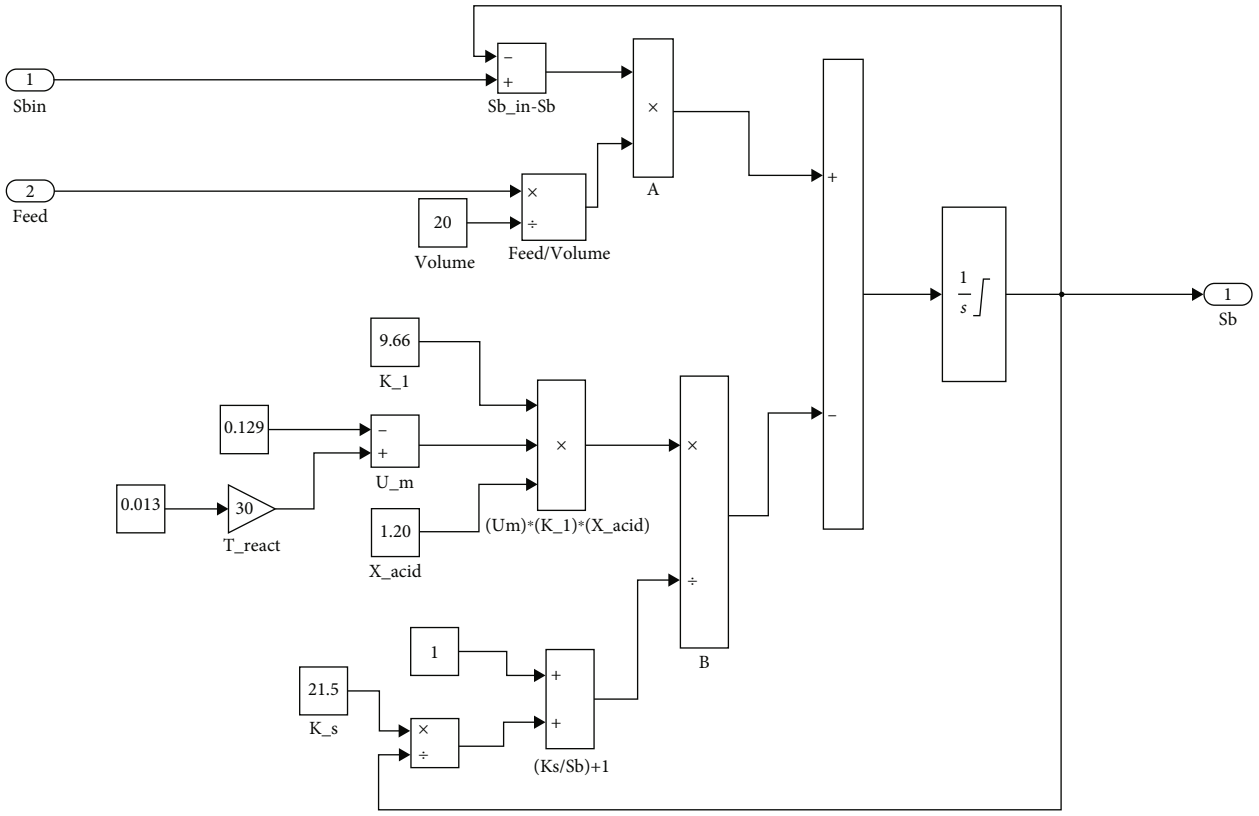

Figure 3: Simulink model of hydrolysis.

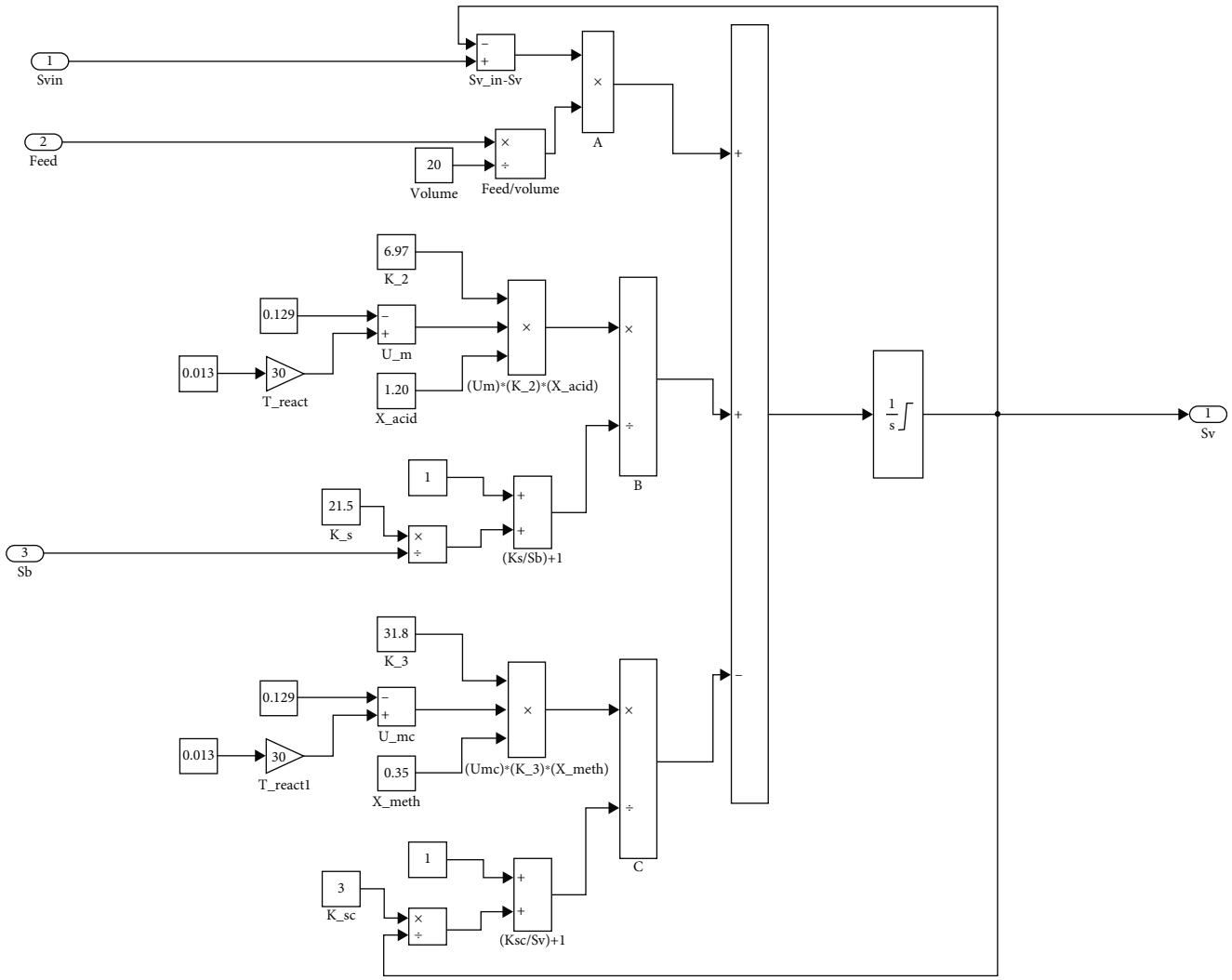

Figure 4: Simulink model of acidogenesis.

the cathode. It owes mainly to a higher current density of anode [43]. The activation loss is given by

$$V_{\text{act}} = \frac{RT}{\alpha nF} \ln\left(\frac{I_{\text{fc}}}{I_o}\right), \tag{13}$$

where α needs to be calculated for respective electrodes and I_{fc} represents fuel cell current. Equation (14) can be preferred as it caters to both electrodes in one equation [43].

$$V_{\text{act}} = (S_A + S_C) \ln\left(\frac{I_{fc}}{i_{o,A}(S_A/S_A + S_C) + i_{o,C}(S_c/S_A + S_C)}\right). \tag{14}$$

3.2.3. Concentration Loss. The implication of the Fick law formula provides concentration loss. This concentration loss is mainly due to reactants dilution by-products. Concentration loss is given by [44]

$$V_{\text{conc}} = \frac{RT}{\alpha nF} \ln\left(1 - \frac{I_{\text{fc}}}{I_l}\right). \tag{15}$$

3.2.4. Ohmic Loss. The internal resistance of the SOFC stack is ohmic resistance, given by

$$V_{\text{ohm}} = I_{fc}R. \tag{16}$$

3.2.5. Other Important Equations for SOFC. The ideal voltage can be given by Equation (17). Moreover, ionic conductivities are given as in [45]

$$E^o = 1.2723 - (2.7645 \times -4).T, \tag{17}$$

$$\sigma_{io,\text{cath}} = \frac{4.2 \times 10^7}{T} e^{(-1200/T)}, \tag{18}$$

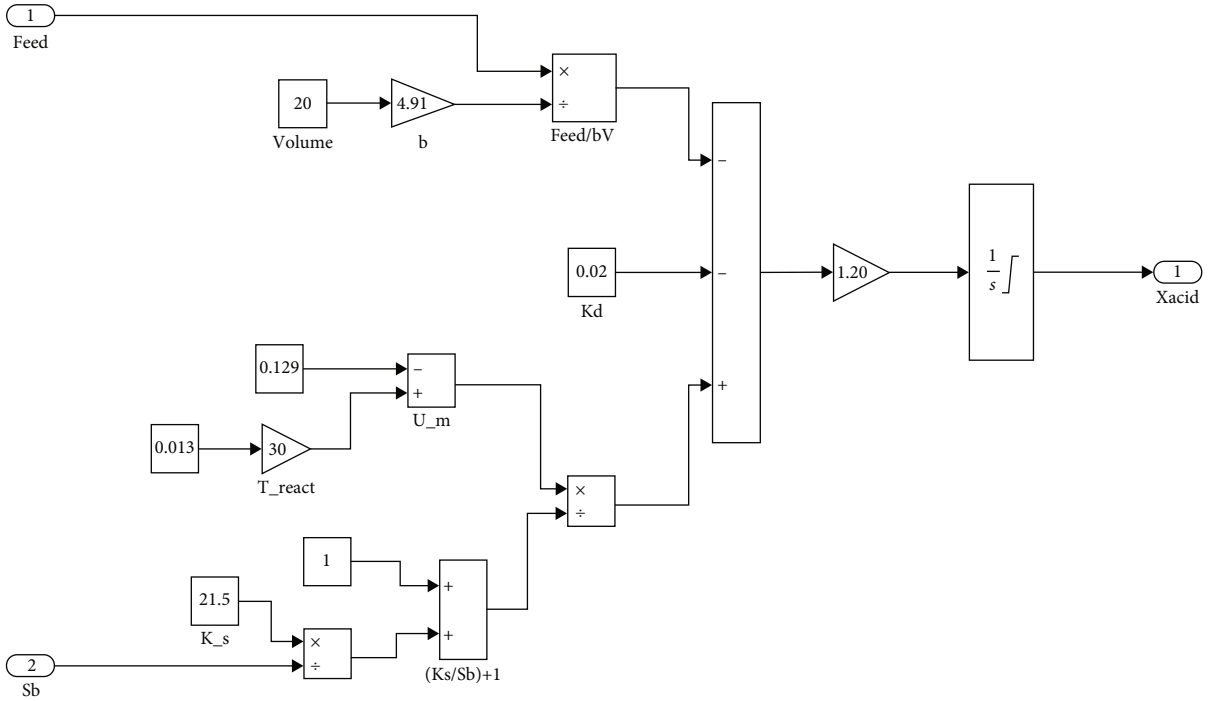

Figure 5: Simulink model of acetogenesis.

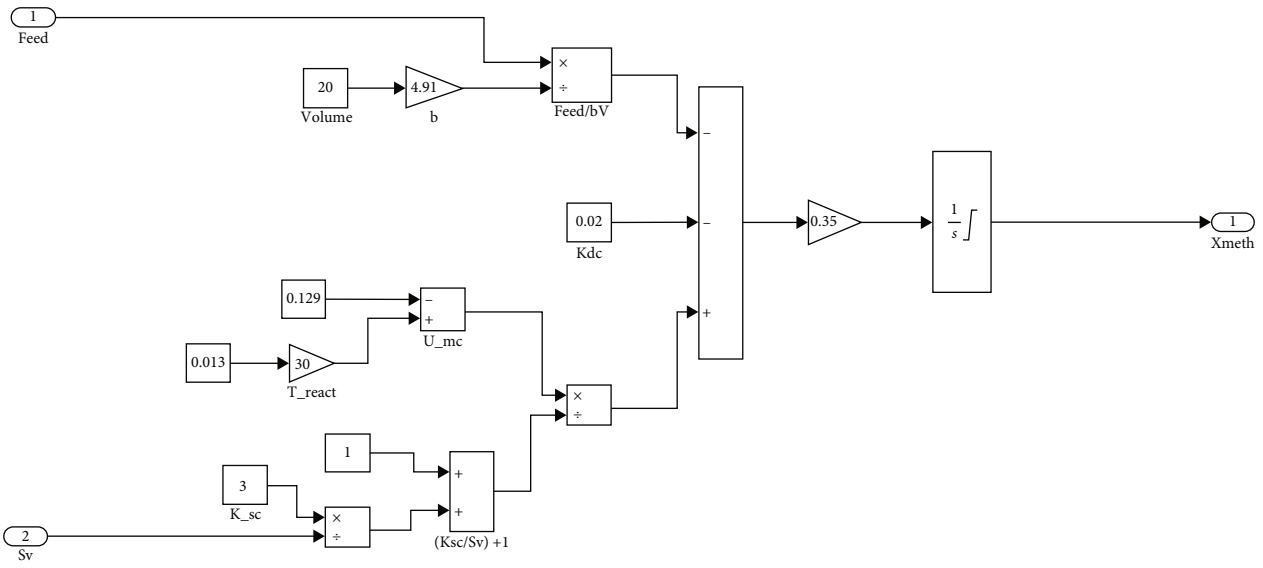

Figure 6: Simulink model of methanogenesis.

$$\sigma_{io,\text{anode}} = \frac{9.5 \times 10^7}{T} e^{(-1150/T)}, \tag{19}$$

$$\sigma_{\text{electrolyte}} = 33.4 \times 10^3 \, e^{(-10{,}300/T)}. \tag{20}$$

3.3. Solar Heating. For solar heating studies, the Hottel Vhiller model (HVM) and Differential Equation model (DEM) are usually adopted. Both models are useful, but the DEM model provides a complex and detailed way to study the solar heating process [46]. Therefore, DEM is adopted for this study. The mathematical model of HVM and DEM is provided in Equation (21) and Equation (22), respectively.

HVM:

$$T_{c,o} = T_a + \frac{I}{k_{aw}} \left(T_{c,i} - T_a - \frac{I}{k_{aw}} \right) e^{(-k_{mw} \cdot A_{\text{solar}}/c.q)}, \tag{21}$$

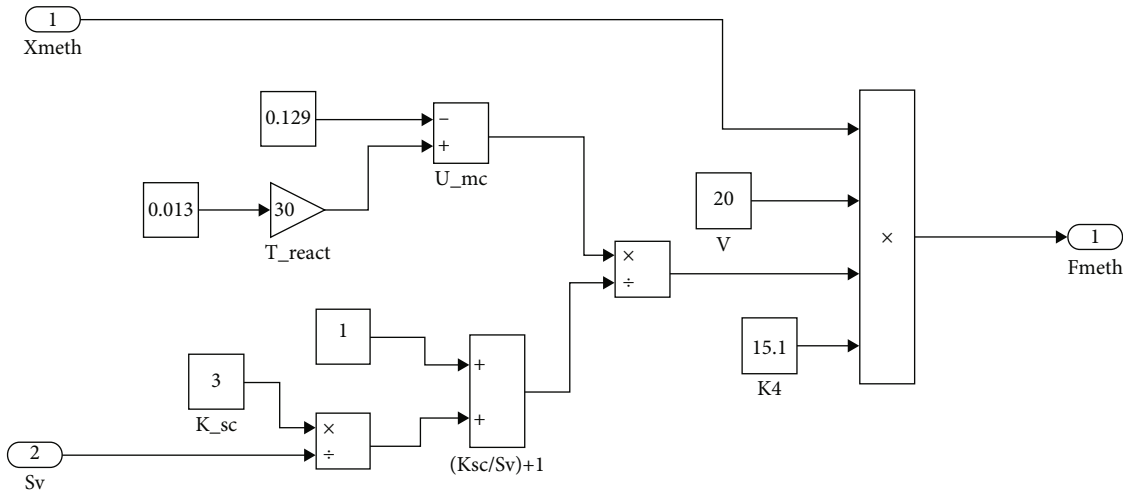

Figure 7: Simulink model for total amount of methane produced.

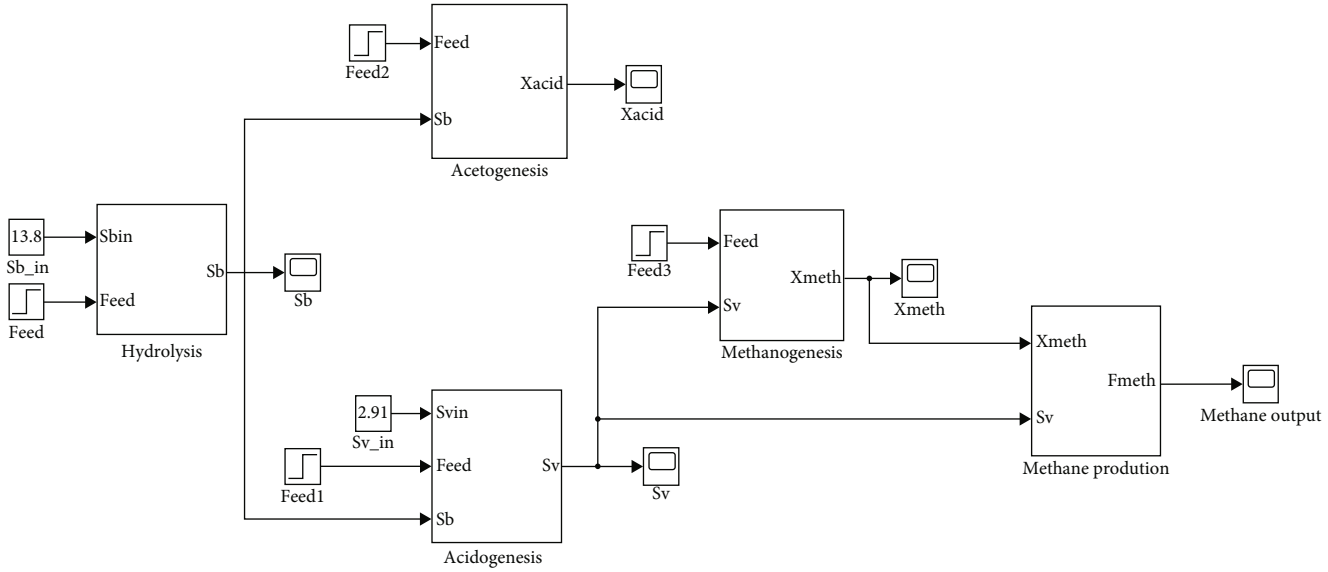

Figure 8: Complete Simulink model of AD.

DEM:

$$T_{c,o} = T_a + \frac{1}{\rho.c.V_{wf}} \int_{\tau_i}^{\tau_f} \left(I.A_{\text{solar}}.\eta + (T_{c,i} - T_{c,o})c.q - \left(T_{\text{avg}} - T_{\text{a}}\right)k.A_{\text{solar}}\right), \quad (22)$$

where

$$T_{\text{avg}} = \frac{T_{c,i} + T_{c,o}}{2}. \quad (23)$$

3.4. Thermal Storage. Thermal energy can be stored in various materials in the form of sensible and latent heat. The sensible heat is associated with the materials that do not change their phase (solid to liquid or gas), and latent heat is associated with phase-changing materials/substances. The amount of thermal energy stored by any medium can be expressed as follows [47, 48].

$$Q_{\text{store}} = \int_{T_i}^{T_f} m.c\, dt. \quad (24)$$

Various solid and liquid materials can be used to store sensible heat, as depicted in Figure 2. Among all, water is the cheapest one [48, 49]. Based on temperature range, magnesia fire bricks are selected for thermal storage.

4. Simulink Model

In this study, MATLAB/Simulink is used for simulation purposes. Based on the mathematical model of AD, SOFC, solar heating, and thermal storage, Simulink models are designed.

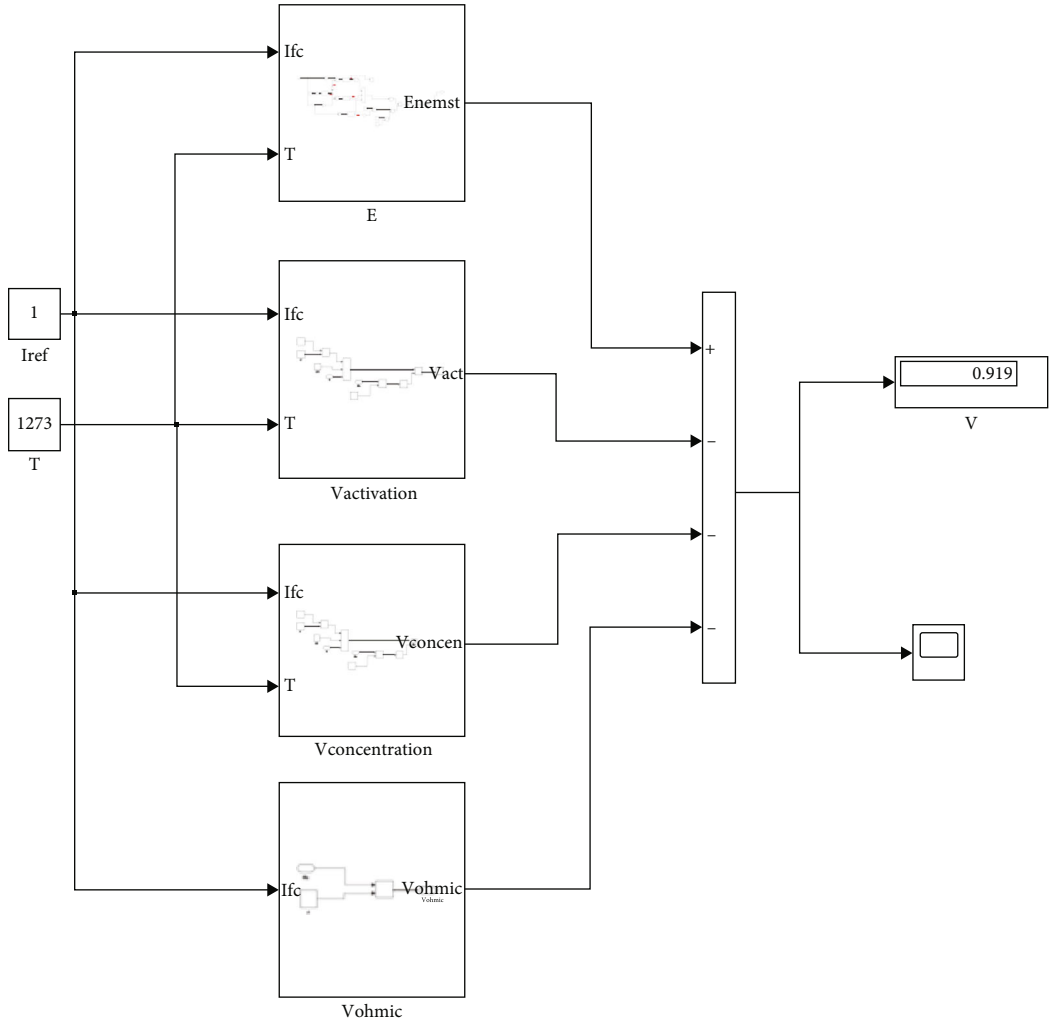

Figure 9: Simulink model of SOFC.

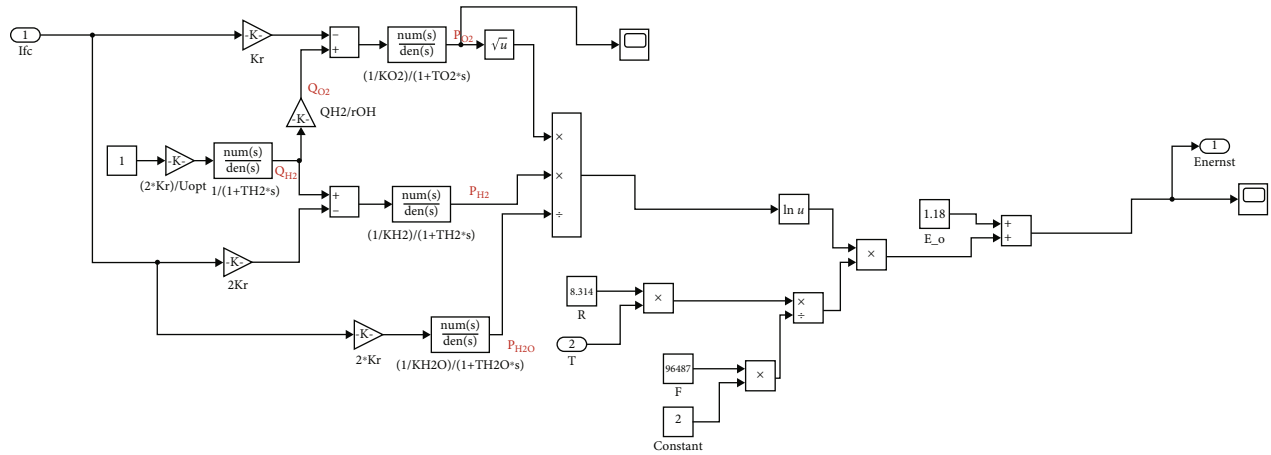

Figure 10: Simulink model for reversible open circuit voltage (E) of SOFC.

4.1. Simulink Model of AD. As AD process, with a 20 m^3 reactor, constitutes four subprocesses (heading 3.1); independent models of these processes are depicted in Figure 3 (hydrolysis), Figure 4 (acidogenesis), Figure 5 (acetogenesis), and Figure 6 (methanogenesis). The model for calculating the total amount of methane produced is

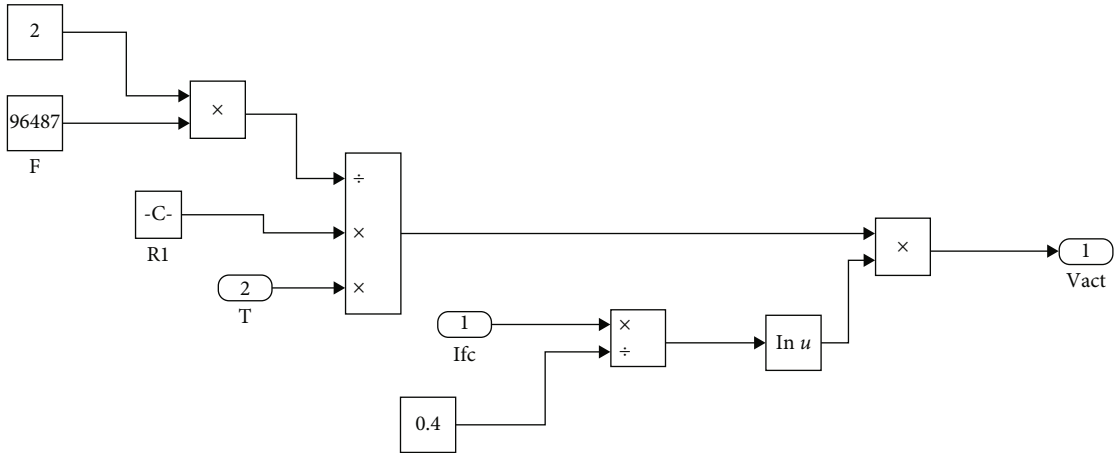

Figure 11: Simulink model for activation loss of SOFC.

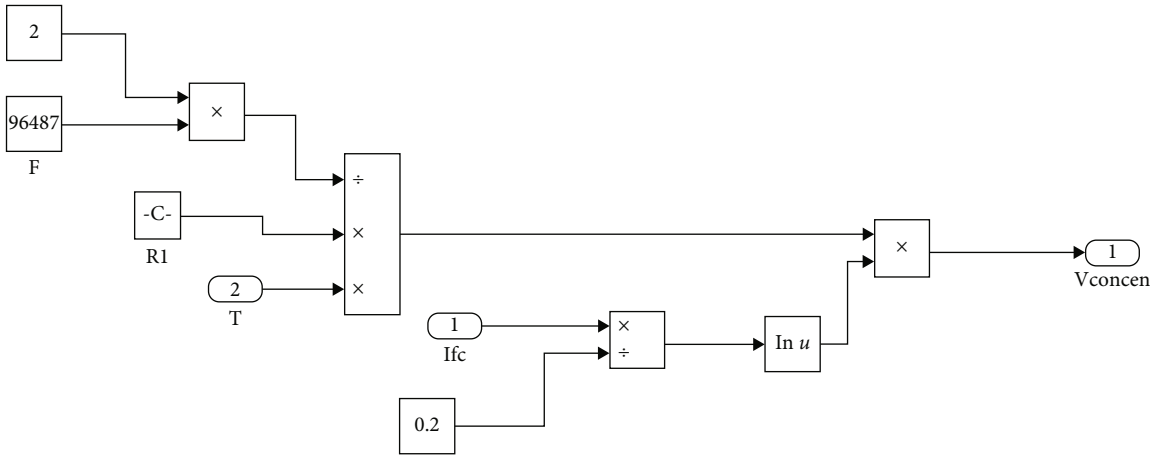

Figure 12: Simulink model for concentration loss of SOFC.

depicted in Figure 7. The complete model with all its components and their correlation is depicted in Figure 8. The data used for simulation purposes is adopted from the literature [40, 51].

4.2. Simulink Model of SOFC. The Simulink model of SOFC is subdivided into four parts to calculate right-hand side parameters of Equation (6), as depicted in Figures 9–13. The parameters are adopted from [52–54]. Figure 9 represents the consolidated model of SOFC, whereas Figures 10–13 represent the subsystems of the consolidated model. Figure 10 calculates the reversible open circuit voltage as given by (7). Figures 11–13 depict different losses associated with SOFC as described by Equations (13)–(16). The system had a voltage of 0.919 V, as shown in Figure 9.

4.3. Simulink Model of Solar Heating. The DEM model is adopted for calculating the exit temperature of a solar heating system as described in Figure 14 and Equation (22). The solar radiation intensity is adopted at 221 Wm^{-2} as an average value for Pakistan [55]. Additional parameters are

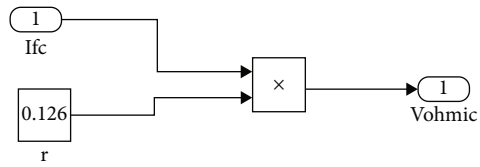

Figure 13: Simulink model for ohmic loss of SOFC.

adopted from [46]. The final Simulink model is described in Figure 14.

4.4. Simulink Model for Thermal Storage. As described earlier, magnesia bricks are adopted for thermal storage. The exhaust temperature of SOFC is much higher in the order of 1273 K; therefore, other materials cannot sustain there. The Simulink model of thermal storage is depicted in Figure 15. The properties of magnesia bricks used in this study are adopted from the reference [48].

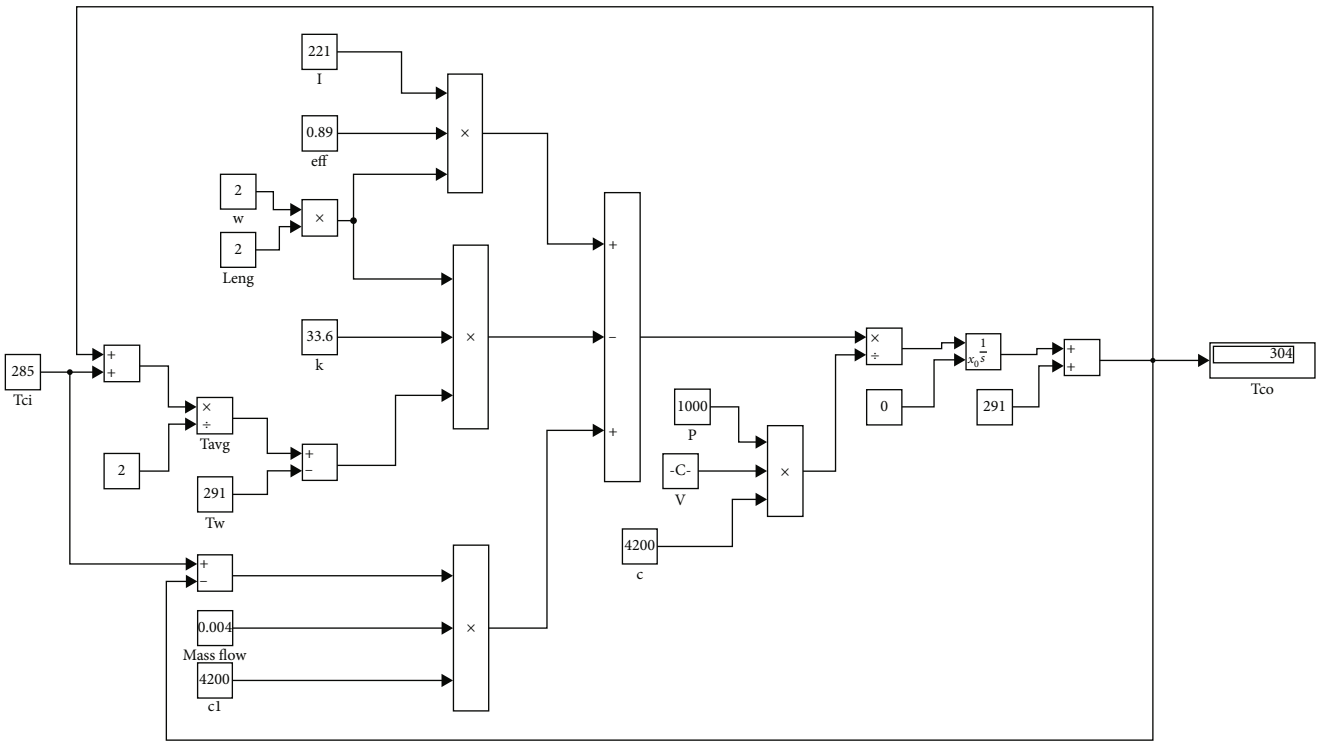

Figure 14: Simulink model of solar heating system.

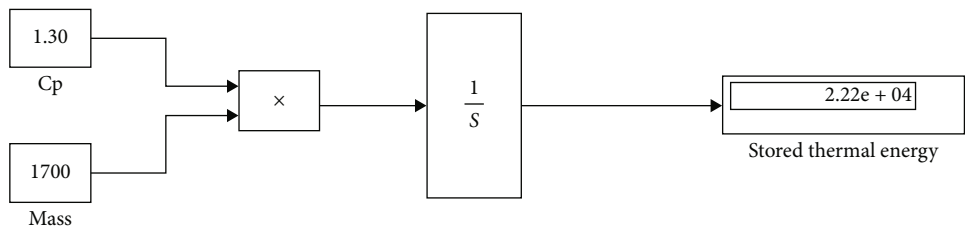

Figure 15: Simulink model of thermal storage.

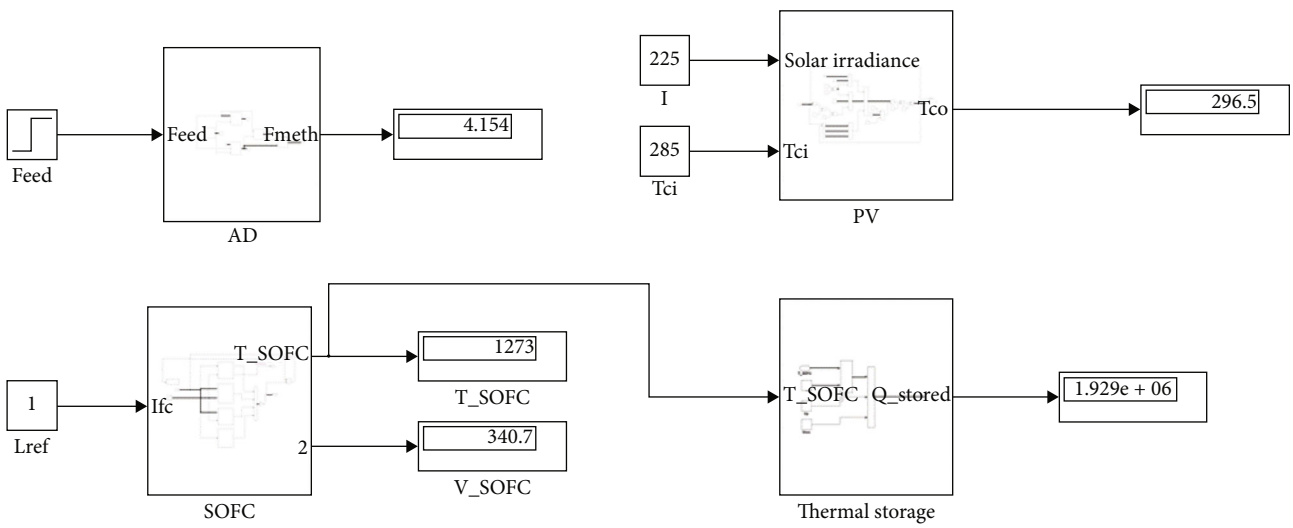

Figure 16: Simulink model of the proposed system.

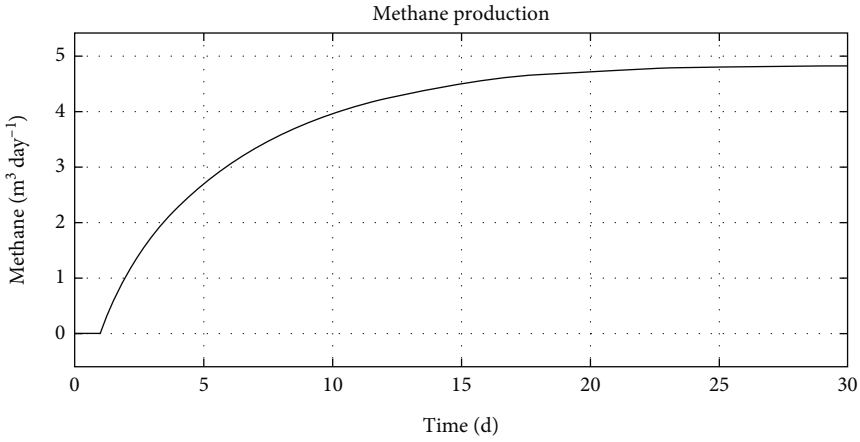

Figure 17: Methane production.

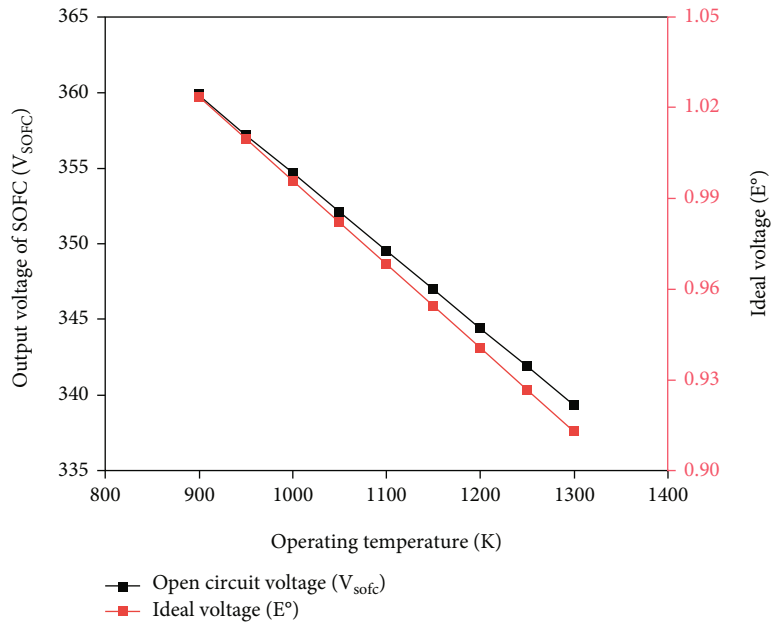

Figure 18: Effect of operating temperature on ideal cell voltage of SOFC (E°) and stack voltage.

4.5. Integrated System. The Simulink model of the complete system is described in Figure 16.

5. Results and Discussion

The AD is fed with poultry manure at the rate of 0.35 m^3day^{-1}. The amount of methane generated by the proposed system is about 4.8 m^3day^{-1}. The amount of methane produced increases in the starting days and then became a constant amount after 20 days, as depicted in Figure 17, plotted based on Figure 8.

The characteristics of SOFC are depicted in Figures 18–21, plotted based on the Simulink model given in Figure 9. SOFC operates at the temperature of 1273 K. The total amount of power produced by the stack of 385 cells amounts to 340.7 W. This electricity can be utilized by residential buildings. No doubt, the amount of electricity produced is far less to meet all energy requirements of any residential area, but it can contribute along with other energy sources. The behavior of SOFC is depicted in Figure 18. The overall voltage of the SOFC decreases as the operating temperature of the SOFC increases. The characteristic curves of SOFC are presented in Figure 19. These curves lie in line with available literature [56]. Figure 20 depicts the effect of the flow rate of hydrogen and oxygen on the overall voltage of the cell. These results are similar to the previous studies [56]. Figure 21 depicts the current density characteristics of SOFC. The efficiency of the SOFC is 73% as it is defined as produced voltage to thermoneutral voltage. In the present case, produced voltage is 0.88 V, and the thermoneutral voltage is 1.2. This efficiency lies in line with the literature [57].

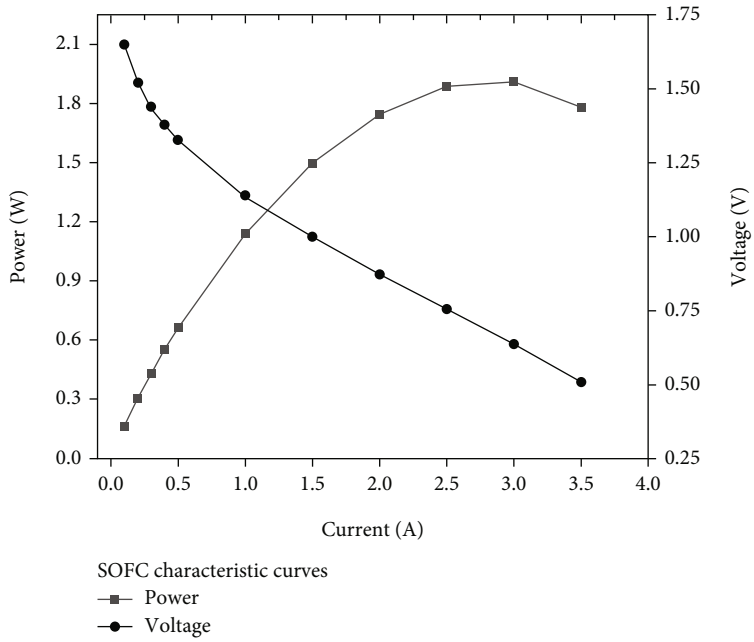

Figure 19: Characteristic curve of SOFC.

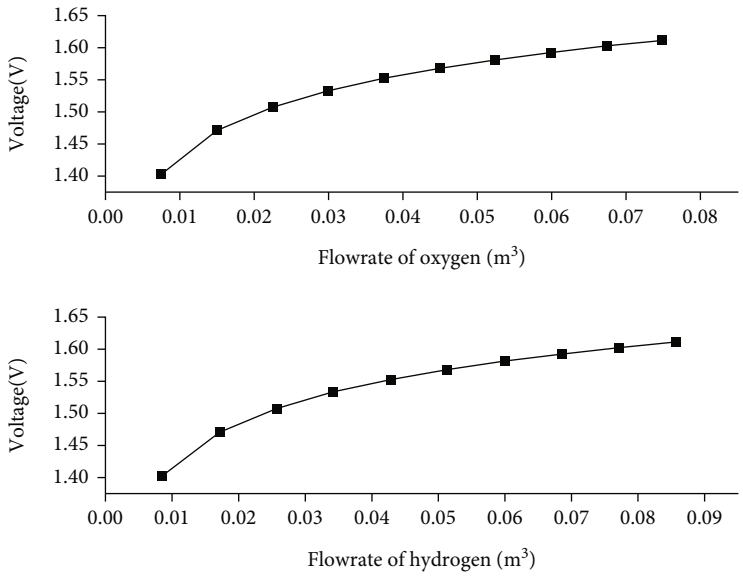

Figure 20: Flow rate effect of SOFC voltage.

6. Possible Applications

The proposed system can find its best applications in cold areas such as Switzerland. These areas require hot water for domestic use all the time. The designed system will ensure the availability of district heating and hot water supply by utilizing the thermal potential of the sun during the day and stored thermal energy (from SOFC) exhaust during nighttime. During the daytime, SOFC exhaust will be completely stored, and during the night, the stored thermal energy will be supplied along with the storage of SOFC exhaust at night. Additionally, the produced methane can be used as transport fuel, and stored CO_2 can be sold to industry. Further, different industrial sectors can adopt the proposed system where heating is a primary concern. Although the proposed system can find its applications in various domestic and industrial scales, practical implications are subjected to feasibility and technoeconomic studies.

Further, as this study provides a Simulink model of the system rather than a traditional thermodynamics analysis, the model can be used for different purposes. First, sensitivity analysis of the cycle, even individual components can be conducted, can be conducted to find parameters that have the highest influence on the cycle output. Second,

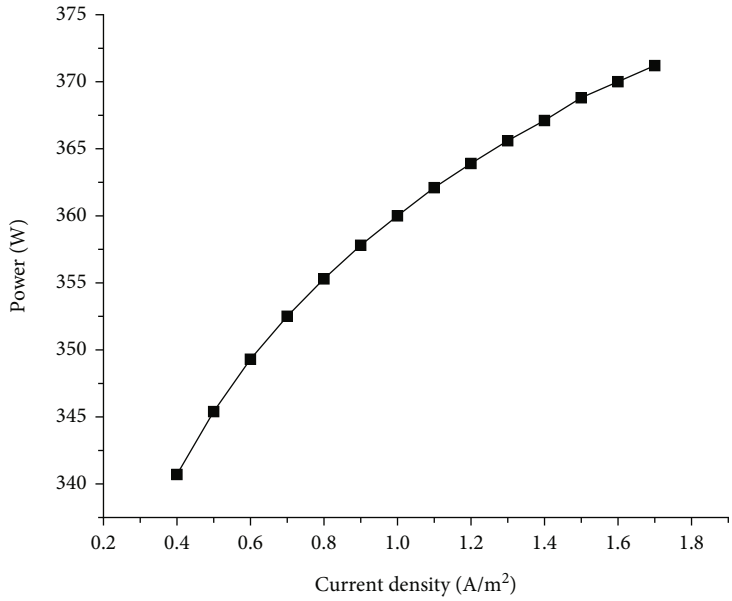

Figure 21: Current density characteristics of SOFC.

optimization studies can be performed using the Simulink model. One such possibility could be using response surface methodology in conjunction with the Simulink model to optimize it. Lastly, the Simulink model can be used to compare one system to another using simulation benchmarking techniques. This will allow authors to compare the performance of different designs or parameters within a system. It is easy to show how certain design choices affect system performance when working with Simulink models.

7. Conclusion

This study contributes to proposing a multigeneration system based on a solid oxide fuel cell powered by an anaerobic digester (AD). AD is fed with animal manure, and methane is produced. The produced methane is fed to SOFC, and excess is used for transport fuel, with 73% efficiency. Thermal energy from the exhaust of SOFC is stored in magnesia bricks. During the daytime, all the exhaust energy is stored, and solar potential is used for the district hot water supply. At night, the stored thermal potential of SOFC is utilized. These types of systems can find their best applications in cold areas that require hot water all over the year. Moreover, all the studies are conducted using MATLAB/Simulink.

In the future, sensitivity analysis of the proposed system can be performed in addition to feasibility analysis. Further, the Simulink model can be used to perform optimization studies, for instance, using the Simulink model in conjunction with response surface methodology could be a suitable option to optimize the proposed system.

Data Availability

No data were used to support this study.

Conflicts of Interest

The authors declare that they have no conflicts of interest.

Acknowledgments

This research is supported by Universiti Brunei Darussalam's university research grant number UBD/RSCH/1.3/FICBF(b)/2019/003.

References

[1] S. Kaza, L. Yao, P. Bhada-Tata, and F. Van Woerden, *What a Waste 2.0: A Global Snapshot of Solid Waste Management to 2050*, The World Bank, 2018.

[2] C. S. Psomopoulos, A. Bourka, and N. J. Themelis, "Waste-to-energy: a review of the status and benefits in USA," *Waste Management*, vol. 29, no. 5, pp. 1718–1724, 2009.

[3] M. M. Siddiqi, M. N. Naseer, Y. Abdul Wahab et al., "Evaluation of municipal solid wastes based energy potential in urban Pakistan," *Processes*, vol. 7, no. 11, p. 848, 2019.

[4] M. S. Khan, Q. Huan, M. Yan, M. Ali, O. U. Noor, and M. Abid, "A novel configuration of solar integrated waste-to-energy incineration plant for multi-generational purpose: an effort for achieving maximum performance," *Renewable Energy*, vol. 194, pp. 604–620, 2022.

[5] M. K. Gupta, P. K. Rakesh, and I. Singh, "Application of industrial waste in metal matrix composite," *Journal of Polymer & Composites*, vol. 4, no. 3, pp. 27–34, 2019.

[6] M. M. Siddiqi, M. N. Naseer, Y. Abdul Wahab et al., "Exploring e-waste resources recovery in household solid waste recycling," *Processes*, vol. 8, no. 9, p. 1047, 2020.

[7] B. K. Ahring, "Perspectives for anaerobic digestion," in *Biomethanation I*, pp. 1–30, Springer, 2003.

[8] D. Nagarajan, D.-J. Lee, and J.-S. Chang, "Integration of anaerobic digestion and microalgal cultivation for digestate

bioremediation and biogas upgrading," *Bioresource Technology*, vol. 290, article 121804, 2019.

[9] H. Li and K. Feng, "Life cycle assessment of the environmental impacts and energy efficiency of an integration of sludge anaerobic digestion and pyrolysis," *Journal of Cleaner Production*, vol. 195, pp. 476–485, 2018.

[10] M. Abid, M. S. Khan, and T. A. H. Ratlamwala, "Thermodynamic performance evaluation of a solar parabolic dish assisted multi-generation system," *Journal of Solar Energy Engineering*, vol. 141, no. 6, 2019.

[11] K. J. Dennis, H. P. Affek, B. H. Passey, D. P. Schrag, and J. M. Eiler, "Defining an absolute reference frame for 'clumped' isotope studies of CO_2," *Geochimica et Cosmochimica Acta*, vol. 75, no. 22, pp. 7117–7131, 2011.

[12] G. Energy, *CO2 status report*, IEA (International Energy Agency), Paris, France, 2019.

[13] E. Tamburini, M. Gaglio, G. Castaldelli, and E. A. Fano, "Biogas from agri-food and agricultural waste can appreciate agroecosystem services: the case study of Emilia Romagna region," *Sustainability*, vol. 12, no. 20, p. 8392, 2020.

[14] E. Martínez-Gutiérrez, "Biogas production from different lignocellulosic biomass sources: advances and perspectives," *3 Biotech*, vol. 8, no. 5, pp. 1–18, 2018.

[15] N.'. A. Yusof, N. Z. Abidin, S. H. M. Zailani, K. Govindan, and M. Iranmanesh, "Linking the environmental practice of construction firms and the environmental behaviour of practitioners in construction projects," *Journal of Cleaner Production*, vol. 121, pp. 64–71, 2016.

[16] M. A. Bagherian and K. Mehranzamir, "A comprehensive review on renewable energy integration for combined heat and power production," *Energy Conversion and Management*, vol. 224, article 113454, 2020.

[17] S. P. Bihari, P. K. Sadhu, K. Sarita et al., "A comprehensive review of microgrid control mechanism and impact assessment for hybrid renewable energy integration," *IEEE Access*, vol. 9, pp. 88942–88958, 2021.

[18] F. Weschenfelder, G. de Novaes Pires Leite, A. C. A. da Costa et al., "A review on the complementarity between grid-connected solar and wind power systems," *Journal of Cleaner Production*, vol. 257, article 120617, 2020.

[19] J. Staniforth and K. Kendall, "Biogas powering a small tubular solid oxide fuel cell," *Journal of Power Sources*, vol. 71, no. 1-2, pp. 275–277, 1998.

[20] V. Adebayo, M. Abid, M. Adedeji, and T. A. H. Ratlamwala, "Energy, exergy and exergo-environmental impact assessment of a solid oxide fuel cell coupled with absorption chiller & cascaded closed loop ORC for multi-generation," *International Journal of Hydrogen Energy*, vol. 47, no. 5, pp. 3248–3265, 2022.

[21] Y. Guo, Z. Yu, G. Li, and H. Zhao, "Performance assessment and optimization of an integrated solid oxide fuel cell-gas turbine cogeneration system," *International Journal of Hydrogen Energy*, vol. 45, no. 35, pp. 17702–17716, 2020.

[22] A. Chitsaz, M. Sadeghi, M. Sadeghi, and E. Ghanbarloo, "Exergoenvironmental comparison of internal reforming against external reforming in a cogeneration system based on solid oxide fuel cell using an evolutionary algorithm," *Energy*, vol. 144, pp. 420–431, 2018.

[23] Y. Xie, Z. Lu, C. Ma et al., "High-performance gas-electricity cogeneration using a direct carbon solid oxide fuel cell fueled by biochar derived from camellia oleifera shells," *International Journal of Hydrogen Energy*, vol. 45, no. 53, pp. 29322–29330, 2020.

[24] J. Van Herle, F. Maréchal, S. Leuenberger, Y. Membrez, O. Bucheli, and D. Favrat, "Process flow model of solid oxide fuel cell system supplied with sewage biogas," *Journal of Power Sources*, vol. 131, no. 1-2, pp. 127–141, 2004.

[25] A. Trendewicz and R. Braun, "Techno-economic analysis of solid oxide fuel cell-based combined heat and power systems for biogas utilization at wastewater treatment facilities," *Journal of Power Sources*, vol. 233, pp. 380–393, 2013.

[26] M. Guillaume, M. S. Bunea, M. Caflisch, M. H. Rittmann-Frank, and J. Martin, "Solar Heat in Industrial Processes in Switzerland - Theoretical Potential and Promising Sectors," in *Proceedings of EuroSun 2018*, pp. 257–267, Rapperswil, 2018.

[27] W. M. Hashim, A. T. Shomran, H. A. Jurmut, T. S. Gaaz, A. A. H. Kadhum, and A. A. Al-Amiery, "Case study on solar water heating for flat plate collector," *Case Studies in Thermal Engineering*, vol. 12, pp. 666–671, 2018.

[28] K. Narula, F. D. O. Filho, J. Chambers, and M. K. Patel, "Simulation and comparative assessment of heating systems with tank thermal energy storage – a swiss case study," *Journal of Energy Storage*, vol. 32, article 101810, 2020.

[29] M. Adedeji, M. Abid, M. Dagbasi, H. Adun, and V. Adebayo, "Improvement of a liquid air energy storage system: investigation of performance analysis for novel ambient air conditioning," *Journal of Energy Storage*, vol. 50, article 104294, 2022.

[30] H. Mahon, D. O'Connor, D. Friedrich, and B. Hughes, "A review of thermal energy storage technologies for seasonal loops," *Energy*, vol. 239, article 122207, 2022.

[31] P. Roos and A. Haselbacher, "Thermocline control through multi-tank thermal-energy storage systems," *Applied Energy*, vol. 281, article 115971, 2021.

[32] B. Singh, Z. Szamosi, and Z. Siménfalvi, "State of the art on mixing in an anaerobic digester: a review," *Renewable Energy*, vol. 141, pp. 922–936, 2019.

[33] A. A. Zaidi, F. RuiZhe, Y. Shi, S. Z. Khan, and K. Mushtaq, "Nanoparticles augmentation on biogas yield from microalgal biomass anaerobic digestion," *International Journal of Hydrogen Energy*, vol. 43, no. 31, pp. 14202–14213, 2018.

[34] R. Z. Feng, A. A. Zaidi, K. Zhang, and Y. Shi, "Optimisation of microwave pretreatment for biogas enhancement through anaerobic digestion of microalgal biomass," *Periodica Polytechnica Chemical Engineering*, vol. 63, no. 1, pp. 65–72, 2018.

[35] F. Haugen, R. Bakke, and B. Lie, "Adapting dynamic mathematical models to a pilot anaerobic digestion reactor," *Modeling, Identification and Control: A Norwegian Research Bulletin*, vol. 34, no. 2, pp. 35–54, 2013.

[36] D. T. Hill, "Simplified monod kinetics of methane fermentation of animal wastes," *Agricultural Wastes*, vol. 5, no. 1, pp. 1–16, 1983.

[37] J. F. Andrews and S. P. Graef, *Dynamic Modeling and Simulation of the Anaerobic Digestion Process*, ACS Publications, 1970.

[38] J. Qu, Y. Sun, M. K. Awasthi et al., "Effect of different aerobic hydrolysis time on the anaerobic digestion characteristics and energy consumption analysis," *Bioresource Technology*, vol. 320, article 124332, 2021.

[39] M. Moo-Young, *Comprehensive Biotechnology*, Elsevier, 2019.

[40] M. Saeed, S. Fawzy, and M. El-Saadawi, "Modeling and simulation of biogas-fueled power system," *International Journal of Green Energy*, vol. 16, no. 2, pp. 125–151, 2019.

[41] I. Angelidaki, D. Karakashev, D. J. Batstone, C. M. Plugge, and A. J. M. Stams, "Biomethanation and its potential," in *Methods in Methane Metabolism, Part A*, vol. 494, pp. 327–351, Elsevier, 2011.

[42] J. Park, D. Kim, J. Baek, Y.-J. Yoon, P.-C. Su, and S. Lee, "Effect of electrolyte thickness on electrochemical reactions and thermo-fluidic characteristics inside a SOFC unit cell," *Energies*, vol. 11, no. 3, p. 473, 2018.

[43] H. Mahcene, H. B. Moussa, H. Bouguetaia, B. Bouchekima, and D. Bechki, "Losses Effect on Solid Oxide Fuel Cell Stack Performance," *Fuel Cells Journal*, 2006.

[44] T. Lakshmi, P. Geethanjali, and P. S. Krishna, "Mathematical modelling of solid oxide fuel cell using Matlab/Simulink," in *2013 Annual International Conference on Emerging Research Areas and 2013 International Conference on Microelectronics, Communications and Renewable Energy*, pp. 1–5, Kanjirapally, India, Jun 2013.

[45] K. Zouhri and S.-Y. Lee, "Exergy study on the effect of material parameters and operating conditions on the anode diffusion polarization of the SOFC," *International Journal of Energy and Environmental Engineering*, vol. 7, no. 2, pp. 211–224, 2016.

[46] J. Tóth and I. Farkas, "Mathematical modelling of solar thermal collectors and storages," *Acta Technologica Agriculturae*, vol. 22, no. 4, pp. 128–133, 2019.

[47] A. Kumar and S. K. Shukla, "A review on thermal energy storage unit for solar thermal power plant application," *Energy Procedia*, vol. 74, pp. 462–469, 2015.

[48] E. C. Okonkwo, M. J. Adedeji, M. Abid, and T. A. H. Ratlamwala, "Thermodynamic analysis of energy storage supported multigeneration system," *Energy Storage*, vol. 1, no. 1, article e33, 2019.

[49] V. Basecq, G. Michaux, C. Inard, and P. Blondeau, "Short-term storage systems of thermal energy for buildings: a review," *Advances in Building Energy Research*, vol. 7, no. 1, pp. 66–119, 2013.

[50] Y. Tian and C.-Y. Zhao, "A review of solar collectors and thermal energy storage in solar thermal applications," *Applied Energy*, vol. 104, pp. 538–553, 2013.

[51] F. Haugen, R. Bakke, and B. Lie, "State estimation and model-based control of a pilot anaerobic digestion reactor," *Journal of Control Science and Engineering*, vol. 2014, Article ID 572621, 19 pages, 2014.

[52] A. Gebregergis, P. Pillay, D. Bhattacharyya, and R. Rengaswemy, "Solid oxide fuel cell modeling," *IEEE Transactions on Industrial Electronics*, vol. 56, no. 1, pp. 139–148, 2009.

[53] A. V. Virkar, Y. Jiang, T. J. Armstrong, F. Zhao, N. Tikekar, and S. Shinde, "Research on SOFC electrodes," in *SECA Workshop*, pp. 18-19, Institute of Electrical and Electronics Engineers,, New York, NY, 2002.

[54] N. Akkinapragada, *Dynamic Modeling and Simulations of Solid Oxide Fuel Cells for Grid-Tied Applications*, University of Missouri–Rolla, 2007.

[55] Z. R. Tahir and M. Asim, "Surface measured solar radiation data and solar energy resource assessment of Pakistan: a review," *Renewable and Sustainable Energy Reviews*, vol. 81, pp. 2839–2861, 2018.

[56] A. F. A. Aziz, A. S. Samosir, K. Kamal, I. Amin, and S. Mathavan, "Modeling and analyzing the proton exchange membrane of fuel cell (PEMFC) in Matlab/SIMULINK environment," in *2011 IEEE 14th International Multitopic Conference*, pp. 238–243, Karachi, Pakistan, 2011.

[57] V. M. Janardhanan, V. Heuveline, and O. Deutschmann, "Performance analysis of a SOFC under direct internal reforming conditions," *Journal of Power Sources*, vol. 172, no. 1, pp. 296–307, 2007.